Available online at www.sciencedirect.com
ScienceDirect
Trans. Nonferrous Met. Soc. China 25(2015) 303−313
Transactions of Nonferrous Metals Society of China
www.tnmsc.cn

# Comparison of electrochemical dissolution of chalcopyrite and bornite in acid culture medium

Hong-bo ZHAO[1,2], Ming-hao HU[1,2], Yi-ni LI[1,2], Shan ZHU[1,2], Wen-qing QIN[1,2], Guan-zhou QIU[1,2], Jun WANG[1,2]

1. School of Minerals Processing and Bioengineering, Central South University, Changsha 410083, China;
2. Key Laboratory of Biohydrometallurgy of Ministry of Education, Central South University, Changsha 410083, China

Received 21 February 2014; accepted 16 July 2014

**Abstract:** The electrochemical dissolution process of chalcopyrite and bornite in acid bacteria culture medium was investigated by electrochemical measurements and X-ray photoelectron spectroscopy (XPS) analysis. Bornite was much easier to be oxidized rather than to be reduced, and chalcopyrite was difficult to be both oxidized and reduced. The relatively higher copper extraction of bornite dissolution can be attributed to its higher oxidation rate. Covellite (CuS) was detected as the intermediate species during the dissolution processes of both bornite and chalcopyrite. Bornite dissolution was preferred to be a direct oxidation pathway, in which bornite was directly oxidized to covellite (CuS) and cupric ions, and the formed covellite (CuS) may inhibit the further dissolution. Chalcopyrite dissolution was preferred to be a continuous reduction−oxidation pathway, in which chalcopyrite was initially reduced to bornite, then oxidized to covellite (CuS), and the initial reduction reaction was the rate-limiting step.

**Key words:** chalcopyrite; bornite; electrochemical dissolution; acid culture medium; bioleaching

## 1 Introduction

Chalcopyrite ($CuFeS_2$) and bornite ($Cu_5FeS_4$) are the most abundant copper-bearing minerals in the world, both having three crystal forms [1,2]. Smelting is still the major process for extracting copper from the two primary copper sulfide minerals [3]. The hydrometallurgical processes, especially the bio-hydrometallurgical processes, have been successfully applied to the processing of secondary copper sulfide minerals, and this technology has a brighter prospect as it is simpler, more efficient and eco-friendly. However, chalcopyrite and bornite are still refractory to bioleaching process, especially under normal temperature (30−35 °C), mainly due to the lack of understanding of the dissolution process during bioleaching [4−6].

Many researchers have studied the reaction mechanisms and rate-determining factors of chalcopyrite dissolution in both bioleaching medium and sole sulfuric acid medium, but different conclusions were obtained. Though most of the researchers attributed the slow rate of chalcopyrite dissolution to its passivation, the specific compositions of passivation film as well as the dissolution process are still being debated. Some researchers identified that metal deficient polysulfide formed during chalcopyrite dissolution can inhibit the further dissolution by controlling the diffusion process of ions [7−9]. However, some others proposed that the passivation should be caused by elemental sulfur and jarosite [10−12].

To investigate the dissolution process of bornite in bioleaching medium or sole sulfuric acid medium, PRICE and CHILTON [13] studied the dissolution process in sulfuric acid by electrochemical, solution, electronic probe, and X-ray diffraction analysis, demonstrating that $Cu_{2.5}FeS_4$ was the stable intermediate. PESIC and OLSON [14] studied the bornite dissolution process in sulfuric acid medium. With the preferential dissolution of iron atoms, iron deficient sulfide ($Cu_5FeS_4$) was identified to be formed first in the inner structure of bornite particles, followed by covellite (CuS) and $Cu_3FeS_4$ on the surface structure and in the inner

**Foundation item:** Projects (51374248, 51320105006) supported by the National Natural Science Foundation of China; Project (NCET-13-0595) supported by the Program for New Century Excellent Talents in University, China; Project (CX2014B091) supported by the Hunan Provincial Innovation Foundation for Postgraduate, China

**Corresponding author:** Jun WANG; Tel: +86-731-88876557; E-mail: wjwq2000@126.com

DOI: 10.1016/S1003-6326(15)63605-6

structure, respectively. BEVILAQUA et al [15] concluded that sulfur and jarosite formed only in the presence of *A. ferrooxidans*, while covellite (CuS) was detected as a secondary phase under all experimental conditions. Some other researchers found that chalcocite and nonstoichiometric copper sulfides also formed during the oxidation and reduction of bornite [16,17].

Chalcopyrite and bornite are associated together most of the time in raw ores, so their interaction and relationship during dissolution process are important topics. Some researchers pointed out that chalcopyrite was reduced to bornite in the initial stage of bioleaching and this first step was also a rate-limiting step [18,19]. ACRES et al [20] found that bornite can decrease the oxidation rate of chalcopyrite, and also slow its leaching rate in hydrochloric acid solution and potassium hydroxide solution. On the contrary, ZHAO et al [21] proposed that a synergistic effect existed between chalcopyrite and bornite bioleaching in the presence of *A. ferrooxidans*.

Moreover, most of the studies were carried out in sole sulfuric acid or in the presence of different strains of bacteria. However, the former ignored the interference of salt compositions in bioleaching medium, and the latter ignored the interference of different bacteria and different chemical substances as the inoculation of bacteria. Therefore, a comparative study on chalcopyrite and bornite dissolution in acid bacteria culture medium was carried out to investigate the dissolution processes of chalcopyrite and bornite. This work will contribute to a deeper understanding of chalcopyrite and bornite dissolution process, as well as their possible interactions during bioleaching.

## 2 Experimental

### 2.1 Electrodes

Chalcopyrite and bornite samples were obtained from Meizhou, Guangdong Province of China. X-ray diffraction analysis showed that they were of extremely high purity. Chemical analysis showed that chalcopyrite contained 34.46% Cu, 31.53% Fe, and 33.12% S (mass fraction), and bornite contained 61.59% Cu, 10.04% Fe, and 27.10% S (mass fraction), respectively. High-purity chalcopyrite and bornite samples were cut into cylinders with diameter of about 1.5 cm, thickness of about 5 mm, with exposed area of 1 $cm^2$. The electrodes were polished using 600-grit metallographic abrasive paper before every electrochemical experiment.

### 2.2 Electrochemical experiments

For all the electrochemical experiments, a conventional three-electrode system consisting of working electrode, graphite rod as counter electrode and Ag/AgCl (3.0 mol/L KCl) electrode as reference electrode was used. The electrolyte of bacterial culture medium was composed of the following compositions: 3.0 g/L $(NH_4)_2{\cdot}SO_4$, 0.1 g/L KCl, 0.5 g/L $K_2HPO_4$, 0.5 g/L $MgSO_4$/L and 0.01 g/L $Ca(NO_3)_2$, with pH value of 1.8 and temperature of 35 °C. The electrochemical experiments were conducted on a Princeton Model 283 potentiostat (EG&G of Princeton Applied Research) coupled to a personal computer.

Cyclic voltammetry measurements were all carried out at a sweep rate of 20 mV/s, and the potentiostatic tests were all performed for the duration of 120 s. All the potentials were expressed with respect to the Ag/AgCl system.

### 2.3 X-ray photoelectron spectroscopy

To investigate the phase transformation of mineral surfaces in the initial stage of dissolution, chalcopyrite and bornite leached in acid culture medium (pH=1.8) for 7 d were analyzed by X-ray photoelectron spectroscopy (XPS). Leached samples were filtered and rinsed with deionized water three times, and then transferred to vacuum drying oven (DZF-6050) to prevent any further oxidation. Finally, dry samples were transferred to the spectrometer in an argon atmosphere before test.

X-ray photoelectron spectroscopy (XPS) measurements were carried out on the model of ESCALAB 250Xi. Spectra were recorded at constant pass energy of 20 eV and energy step size of 0.1 eV, with Al $K_\alpha$ X-ray as source. Binding energy calibration was based on C 1s at 284.6 eV. XPS PEAK 4.1 software was used for fitting the XPS peaks.

## 3 Results and discussion

### 3.1 Cyclic voltammetry experiments

Figure 1 shows the cyclic voltammograms of chalcopyrite and bornite electrodes in two different scan routes. The positive scan route started scanning towards anodic direction, then reversed to cathodic direction, and finally switched towards anodic direction again. The negative scan route started scanning towards cathodic direction, then switched towards anodic direction, and finally reversed to cathodic direction. Figure 1(a) shows the cyclic voltammograms of chalcopyrite electrode scanning from 0.3 V. Distinct differences can be found between the positive and negative scan route. The corresponding reactions of each peak according to the other researches were summarized as follows.

Peak 1 appearing in the range of 0 to 0.3 V was only detected significantly in the positive scan route.

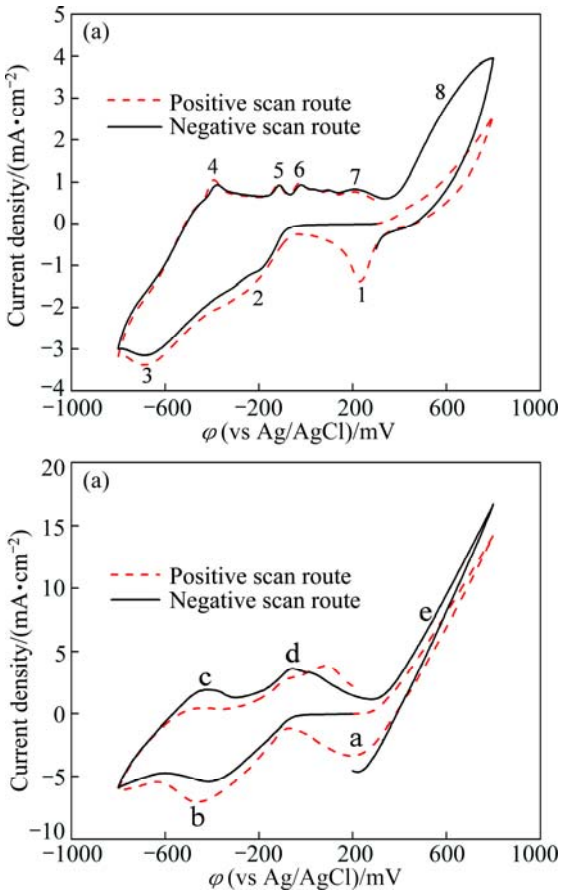


**Fig. 1** Cyclic voltammograms of chalcopyrite and bornite electrodes in different scan routes: (a) Chalcopyrite; (b) Bornite

This peak was described by many researchers using Eqs. (1) to (8) [19,22−25]:

$$Cu^{2+} + S^0 + 2e^- \rightarrow CuS \quad (1)$$

$$Cu^{2+} + CuS + 2e^- \rightarrow Cu_2S \quad (2)$$

$$2CuS + 2H^+ + 2e^- \rightarrow Cu_2S + H_2S \quad (3)$$

$$Cu^{2+} + 2e^- \rightarrow Cu^0 \quad (4)$$

$$CuFeS_2 + 3Cu^{2+} + 4e^- \rightarrow Cu_5FeS_4 + Fe^{2+} \quad (5)$$

$$CuFeS_2 + 3Cu^{2+} + 4e^- \rightarrow 2Cu_2S + Fe^{2+} \quad (6)$$

$$9CuFeS_2 + 4H^+ + 2e^- \rightarrow Cu_9Fe_8S_{16} + 2H_2S + Fe^{2+} \quad (7)$$

$$5CuFeS_2 + 12H^+ + 4e^- \rightarrow Cu_5FeS_4 + 6H_2S + 4Fe^{2+} \quad (8)$$

Peak 2 was mainly attributed to the reactions of Eqs. (9) and (10) as reported in Refs. [19,22−24]:

$$2CuFeS_2 + 6H^+ + 2e^- \rightarrow Cu_2S + 2Fe^{2+} + 3H_2S \quad (9)$$

$$S^0 + 2H^+ + 2e^- \rightarrow H_2S \quad (10)$$

Peak 3 was mainly associated with the reactions of Eqs. (11) and (12) as [19,22−24]:

$$2CuFeS_2 + 4H^+ + 2e^- \rightarrow Cu^0 + 2H_2S + Fe^{2+} \quad (11)$$

$$Cu_2S + 2H^+ + 2e^- \rightarrow 2Cu^0 + H_2S \quad (12)$$

In the anodic scan from −0.8 V to 0.8 V, five anodic peaks can be detected in both of the two cyclic voltammograms. Peak 4 was attributed to the oxidation reactions of metal copper to chalcocite ($Cu_2S$) according to Eq. (13) [19,22−24]:

$$2Cu^0 + H_2S \rightarrow Cu_2S + 2H^+ + 2e^- \quad (13)$$

For the following continuous anodic peaks named peak 5 and peak 6, the possible reactions were summarized as Eqs. (14) and (15) [19,22−24]:

$$H_2S \rightarrow S^0 + 2H^+ + 2e^- \quad (14)$$

$$CuFeS_2 \rightarrow CuS + S^0 + Fe^{2+} + 2e^- \quad (15)$$

Peak 7 was commonly considered the oxidation of chacocite ($Cu_2S$) to a series of sulfides, including djurleite ($Cu_{1.92}S$), digenite ($Cu_{1.60}S$) and covellite (CuS) as shown in Eq. (16) [19,22−24]:

$$Cu_2S \rightarrow Cu_xS + (2-x)Cu^{2+} + (4-2x)e^- \quad (16)$$

The pre-wave of peak 8 can represent the oxidation reactions as shown in Eq. (17) to Eq. (19) [19,22−24]:

$$CuFeS_2 \rightarrow Cu_{1-x}Fe_{1-y}S_{2-z} + xCu^{2+} + yFe^{2+} + zS^0 + 2(x+y)e^- \quad (17)$$

$$CuS \rightarrow Cu^{2+} + S^0 + 2e^- \quad (18)$$

$$2CuFeS_2 + 5H_2O \rightarrow 2CuO + Fe_2O_3 + 4S^0 + 10H^+ + 10e^- \quad (19)$$

It is evident that higher current density of peak 8 during negative scan route can be detected. Peak 8 was in the potential range of about 0.3 V to 0.8 V, where the main oxidation reactions of releasing $Cu^{2+}$ ions took place, indicating that the dissolution of chalcopyrite can be significantly accelerated due to the reduction reactions. The evident cathodic peak 1 detected during positive scan route can be mainly attributed to the higher rate of reduction reactions with $Cu^{2+}$ ions involved, which should be released by the direct oxidation process during the anodic scan.

The cyclic voltammograms of bornite electrode scanning from 0.2 V is shown in Fig. 1(b). The possible reactions were summarized as follows according to the other research.

Peak a can only be significantly detected in the positive scan route, and it mainly represented the reactions of Eq. (1) to Eq. (4) mentioned above. Peak b occurred in both of the two curves, and this peak was mainly attributed to the reactions of Eqs. (10), (12) and (20). Similarly, peak c and peak d detected can be

associated with the reactions of Eqs. (13) and (14), respectively. However, when the potential was more than 0.25 V (vs SCE), the following reactions of Eq. (21) to Eq. (23) can take place [13,24−26].

$$3Cu_5FeS_4 + 6H^+ + 2e^- \rightarrow 5Cu_2S + 3H_2S + 2Fe^{2+} \quad (20)$$

$$Cu_5FeS_4 \rightarrow Cu_{5-x}FeS_4 + xCu^{2+} + 2xe^- \quad (21)$$

$$Cu_{5-x}FeS_4 + 6H^+ \rightarrow CuS + (4-x)Cu^{2+} + 3H_2S + Fe^{3+} + (5-2x)e^- \quad (22)$$

$$Cu_{5-x}FeS_4 \rightarrow (5-x)Cu^{2+} + Fe^{3+} + 4S^0 + (13-2x)e^- \quad (23)$$

The $Cu^{2+}$ ions were released in the direct oxidation process, thus accelerating the reduction reactions corresponding to peak a. However, the current densities of peak e in the two curves were similar, verifying that the reduction of bornite had no obvious influence on its further dissolution.

During the negative scan route, the effects of initial scan potentials on the electrochemical behaviors of chalcopyrite and bornite electrodes are shown in Fig. 2. Figure 2(a) shows that the current densities of anodic peaks in the range of 0.3 V to 0.8 V increased with increasing initial scan potential, indicating that a higher initial scan potential in negative scan route was beneficial to the oxidation of chalcopyrite. This can be mainly because of the accelerated reduction reactions and the accumulated reduzate during the cathodic scan in a wider scan potential range. For the electrochemical behaviors of bornite shown in Fig. 2(b), it can be found that the two patterns were similar except for the cathodic peak around 0.2 V, where the reduction reactions were accelerated as the $Cu^{2+}$ ions releasing at a higher potential. Therefore, the further dissolution of bornite during the negative scan route was neglectfully influenced by the initial scan potential or the initial reduction.

Figure 3(a) reveals that no specific relationship between the initial scan potential and electrochemical behaviors of chalcopyrite existed in the positive scan route. The four similar curves indicated that chalcopyrite was difficult to be oxidized even in a relatively higher potential. While for cyclic voltammograms of bornite shown in Fig. 3(b), the direct oxidation reactions in the potential range of 0.2 to 0.8 V were significantly accelerated with the increase of initial scan potential. Additionally, the rate of reduction reactions increased with increasing initial scan potential. Therefore, a relatively higher potential can enhance the oxidation of bornite significantly.

Comparative results of the cyclic voltammograms of chalcopyrite and bornite electrodes are shown in Fig. 4. Their respective anodic and cathodic peaks appeared almost in the same potential ranges, indicating

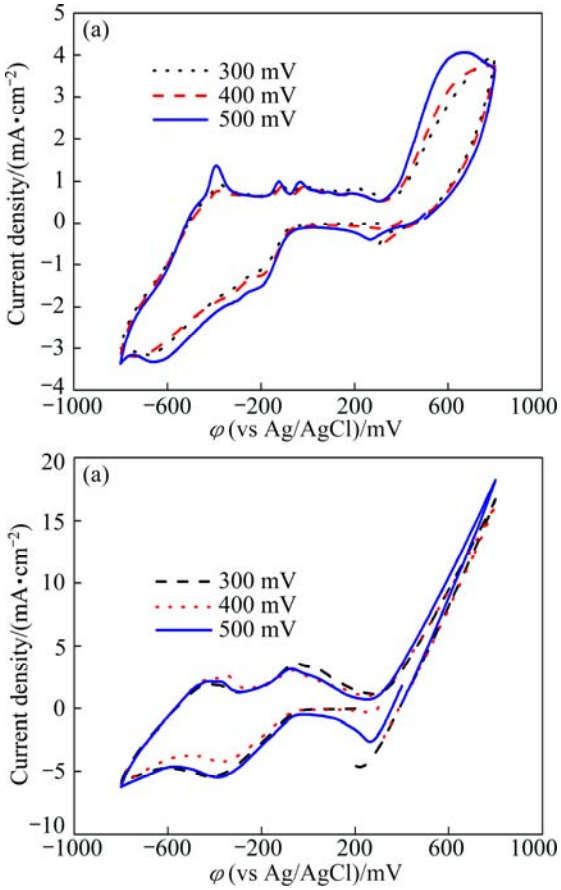


**Fig. 2** Cyclic voltammograms of chalcopyrite and bornite electrodes in negative scan route at different initial scan potentials: (a) Chalcopyrite; (b) Bornite

that similar oxidation and reduction reactions took place during the electrochemical dissolution processes of chalcopyrite and bornite. This implies that the dissolution process of chalcopyrite may contain the dissolution process of bornite, as reported by some other researchers [18,19,27]. However, the current density of almost every peak of bornite electrode was higher than that of chalcopyrite, verifying that the reaction rates of both oxidation and reduction reactions of bornite were higher than those of chalcopyrite in acid culture medium.

### 3.2 Potentiostatic tests

To characterize the potential range where oxidation and reduction reactions of dissolution process took place, potentiostatic experiments were performed in different potential ranges. Figure 5 shows the relationship between time and current density of chalcopyrite electrode. It reveals that the potential range of less than 0.2 V was the region of reduction reactions, and the oxidation reactions took place in the potential range of more than 0.3 V. Moreover, the current density increased with the decrease of applied potential in the reduction region, while it was contrary in the oxidation region.

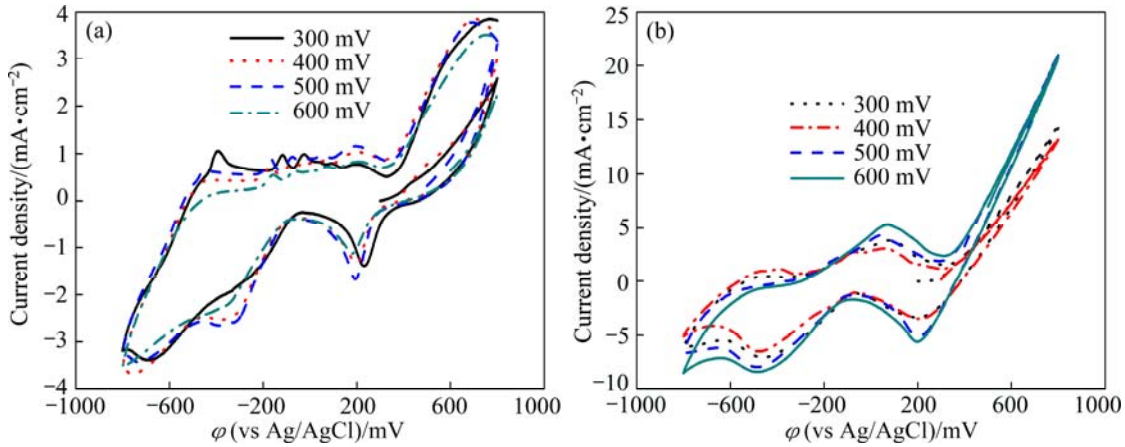


**Fig. 3** Cyclic voltammograms of chalcopyrite and bornite electrodes in positive scan route at different initial scan potentials: (a) Chalcopyrite; (b) Bornite

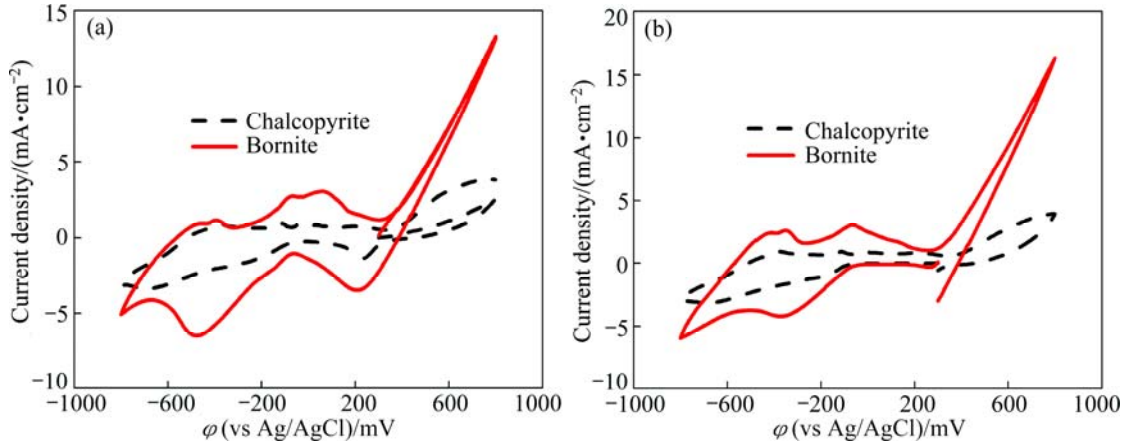


**Fig. 4** Comparison of cyclic voltammograms of chalcopyrite and bornite electrodes in acid culture medium: (a) Positive scan route; (b) Negative scan route

The relationship between time and current density of bornite electrode is shown in Fig. 6, which indicates that the reduction reactions of bornite took place in the potential range of less than 0.2 V, and the region of oxidation reactions was in the potential range of more than 0.3 V. Similarly, the current density increased with the decrease of applied potential in the reduction region, and contrary in the oxidation region.

The total charges evaluated by the integral of current density and time of the potentiostatic tests can represent the corresponding reaction rate at a certain potential. The relationship between the total charges and applied potential is shown in Fig. 7. For the chalcopyrite dissolution process, Fig. 7(a) shows that three different regions existed from −0.6 V to 0.7 V, the smallest slop in the region I (0−0.4 V) indicates that the reactions in this potential range should be the main rate limiting step during chalcopyrite dissolution process. This range was also the main potential range during the initial stage of chalcopyrite bioleaching. Therefore, the slow rate of both oxidation and reduction reactions contributed to the slow dissolution rate of chalcopyrite.

The relationship between total charges and applied potential during bornite dissolution process is shown in Fig. 7(b). This reveals that the reduction reactions in the region I should be the main rate limiting step, and the direct oxidation reactions should be the fastest as shown in the region III.

Figure 8(a) shows the total charges of chalcopyrite and bonite in oxidation region and reduction region, respectively. The direct oxidation rate of bornite was significantly higher than that of chalcopyrite. This should account for the higher dissolution rate of bornite during leaching process. While for the reduction region shown in Fig. 8(b), the total charges of both chalcopyrite and bornite in the potential range of 0 V to 0.2 V were very low, indicating that the reduction reactions rates of chalcopyrite and bornite during dissolution were very slow. When the potential was less than 0 V, bornite can be easier to reduce than chalcopyrite.

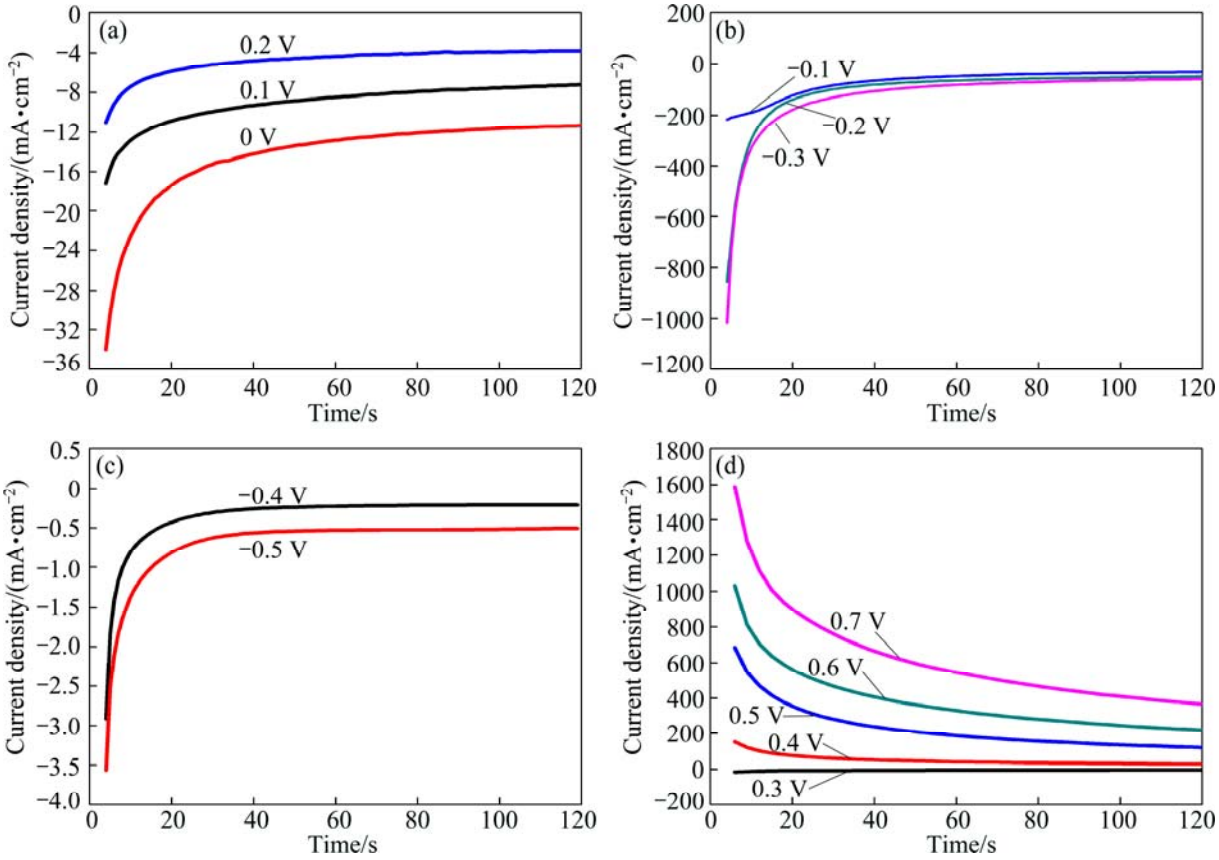


**Fig. 5** Current density−time curves of chalcopyrite electrode at different applied potentials for 120 s

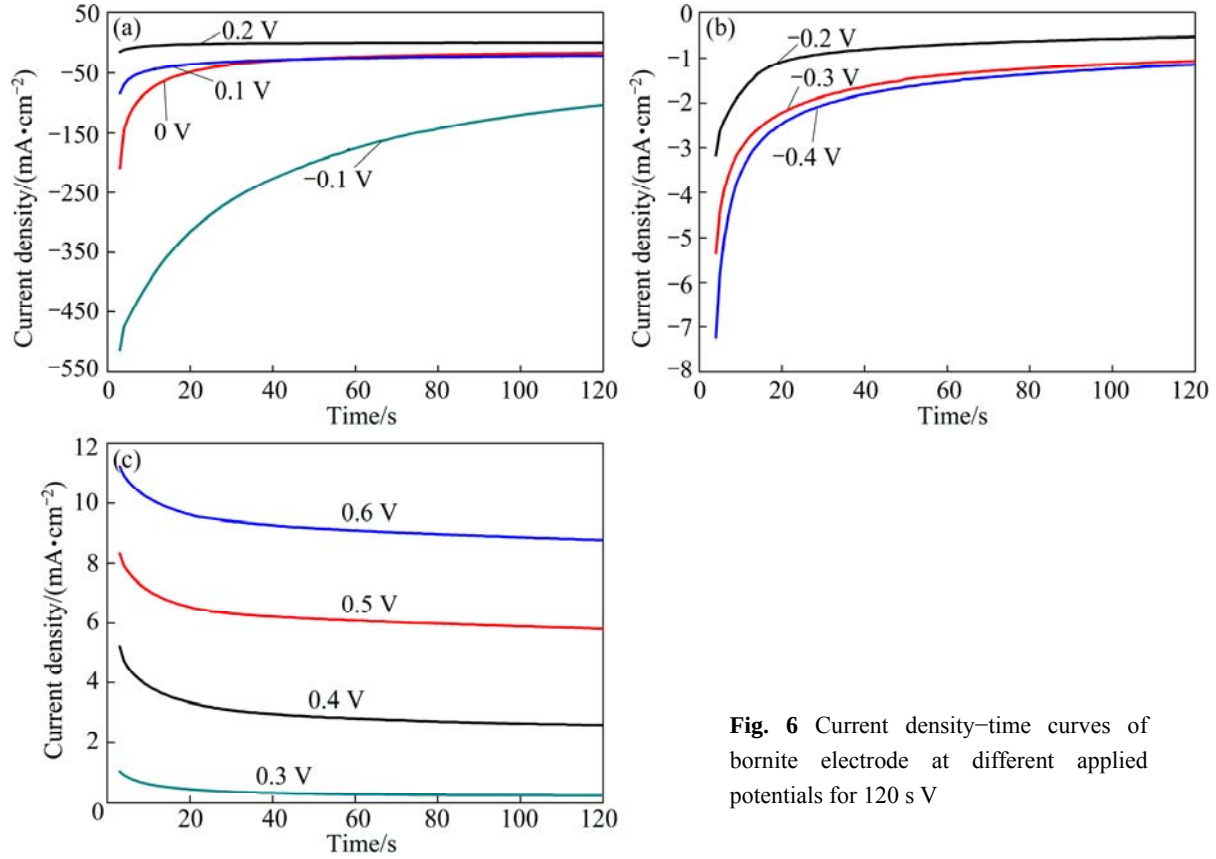


**Fig. 6** Current density−time curves of bornite electrode at different applied potentials for 120 s V

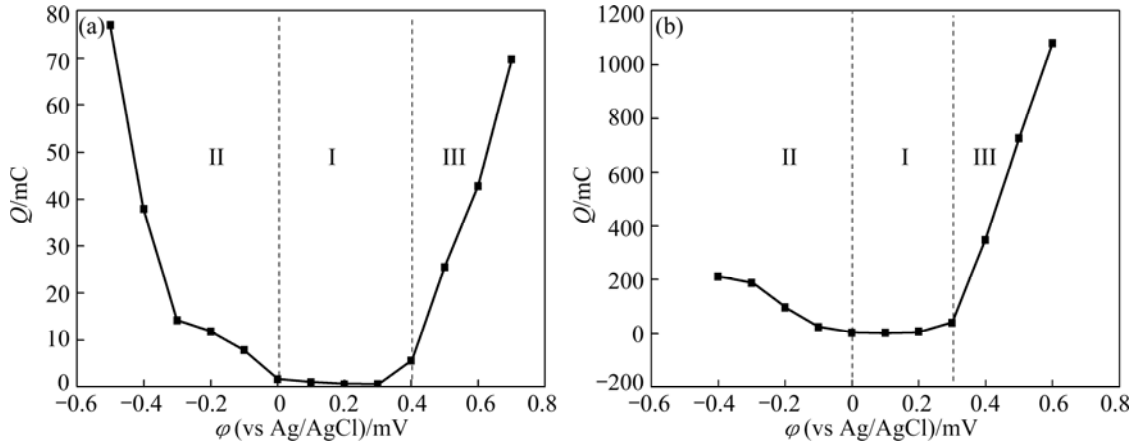


**Fig. 7** Relationship between total charges (evaluated from current density−time curves) and applied potential: (a) Chalcopyrite; (b) Bornite

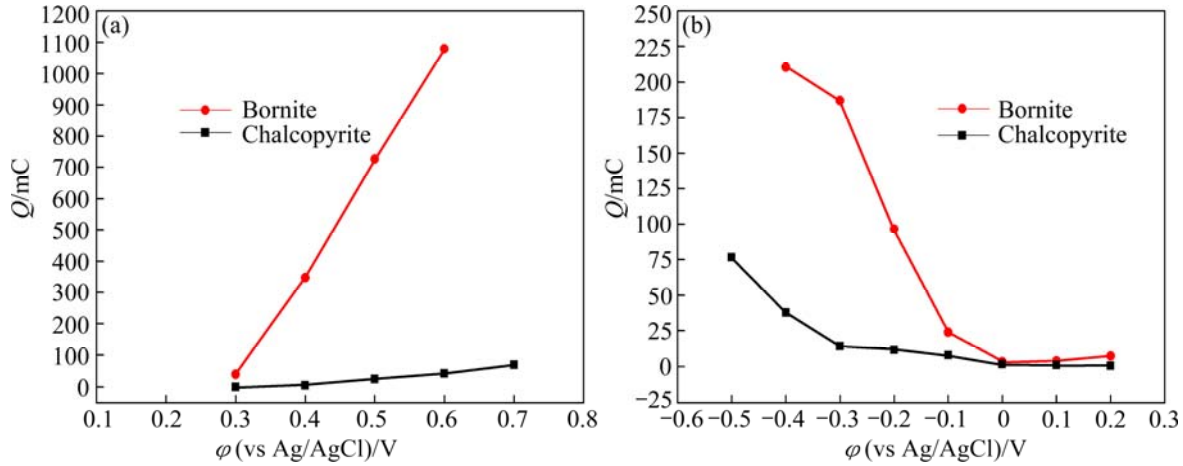


**Fig. 8** Comparison of total charges between chalcopyrite and bornite electrode in oxidation range and reduction range: (a) Oxidation range; (b) Reduction range

### 3.3 XPS analysis

The dissolution process can be described as a superficial corrosion process, during which mineral surfaces can be reconstructed to form very thin layer of new compounds. XPS can provide reliable data on the chemical states of the mineral surface, and it can help to investigate the intermediate species during dissolution process. The initial step of dissolution of chalcopyrite and bornite is vital for the further dissolution. Additionally, chalcopyrite and bornite dissolved fast in the initial stage, but slower in the later stage because of the passivation. Therefore, the characterization of the intermediate species in the initial stage of dissolution can contribute to the study of dissolution pathways of chalcopyrite and bornite. XPS spectra of chalcopyrite and bornite leached in acid culture medium for 7 d are shown in Fig. 9.

Figure 9(a) presents the Cu 2p peaks of the above two samples. It shows that the peaks of leached chalcopyrite and leached bornite were almost the same. The two peaks should be the Cu $2p_{3/2}$ and Cu $2p_{1/2}$, and they were centered at about 932.4 and 952.2 eV, respectively. It has been well demonstrated that Cu $2p_{3/2}$ peak with binding energy of 933.0−933.8 eV and the presence of a shake-up peak at 939−944 eV were the two major XPS characteristics of cupric species, while a lower Cu $2p_{3/2}$ binding energy (about 931.8−933.1 eV) and the absence of the shake-up peak were the characteristics of cuprous species, including cuprous oxide ($Cu_2O$) and cuprous sulfide (CuS and $Cu_2S$). The Cu $2p_{3/2}$ peaks of $Cu_2O$, $Cu_2S$ and CuS were reported to be centered at 932.8, 932.6 and 932.0 eV, respectively [7,28]. The Cu LMM peaks of the four samples are shown in Fig. 9(b), which reveals that the Cu LMM peaks of leached chalcopyrite and bornite were almost the same, and they were centered at about 568.7 eV. The corresponding values of $Cu_2O$, $Cu_2S$ and CuS were 569.7, 569.5 and 568.5 eV, respectively [7,20,28,29]. Therefore, covellite (CuS) can be the most plausible cuprous species during the dissolution process of chalcopyrite and bornite.

Figure 9(c) shows the S 2p XPS spectra of leached

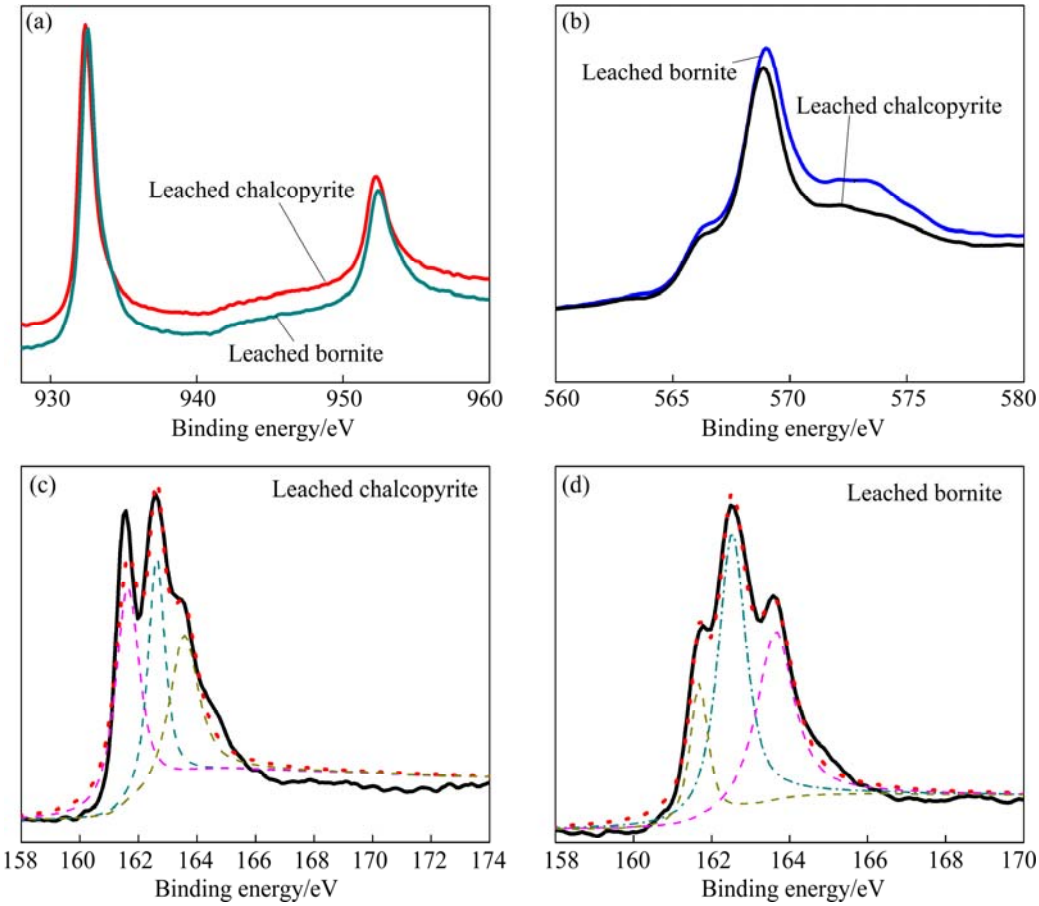


**Fig. 9** XPS spectra of leached chalcopyrite and leached bornite in acid 9K medium for 7 d: (a) Cu 2p peaks; (b) Cu LMM peaks; (c) S 2p peaks; (d) S $2p_{3/2}$ peaks

chalcopyrite. The first S $2p_{3/2}$ peak at about 161.6 eV was in agreement with the value of monosulfide ($S^{2-}$) sulfur species (161.1−161.8 eV), including covellite (CuS) or iron sulfides (FeS) [30,31]. The second S $2p_{3/2}$ peak was with the binding energy of 162.5 eV, which was in consistence with the value of disulfide ($S_2^{2-}$) sulfur species of covellite (CuS) and iron disulfide ($FeS_2$) [32,33]. Additionally, one more peak centered at the binding energy of about 163.5 eV agreed well with the peak position of polysulfide species ($S_n^{2-}$) [7,34]. However, the main peaks of S $2p_{3/2}$ were centered at 161.6 and 162.5 eV, respectively. Therefore, covellite (CuS), with the most probable formulation of $Cu_3^+S_2^{2-}S^-$, can be the main intermediate species during chalcopyrite dissolution in acid culture medium.

Figure 9(d) shows the S $2p_{3/2}$ core level peak of leached bornite. The first S $2p_{3/2}$ peak centered at 161.6 eV and the second S $2p_{3/2}$ peak centered at about 162.5 eV indicate that covellite (CuS) can be the main intermediate species during bornite dissolution in acid culture medium. Additionally, one obvious peak centered at 163.6 eV indicates that significant amount of polysulfide species also formed on bornite surface.

From the analysis of XPS spectra above, covellite (CuS) was determined to be the main intermediate species during both chalcopyrite and bornite dissolution in acid culture medium. Polysulfide also formed on the chalcopyrite and bornite surface.

### 3.4 Discussion on dissolution pathway of chalcopyrite and bornite

Figure 10 shows the possible dissolution pathways of chalcopyrite and bornite in acid culture medium according to the current work and some other researches.

For the bornite dissolution process in acid culture medium, the first dissolution pathway was a continuous reduction and oxidation process, in which bornite was reduced to chalcocite ($Cu_2S$), and then oxidized. In the other dissolution pathway, bornite was directly oxidized to covellite (CuS) and cupric ions. However, the electrochemical analysis reveals that the reduction reaction of bornite was very difficult. Moreover, XPS analysis results also suggested that covellite (CuS) formed in the initial stage of bornite dissolution. Therefore, the pathway of direct oxidation should be preferred in this work. As covellite (CuS) can only be oxidized in a relatively high redox potential, the formed covellite (CuS) can inhibit the further dissolution of

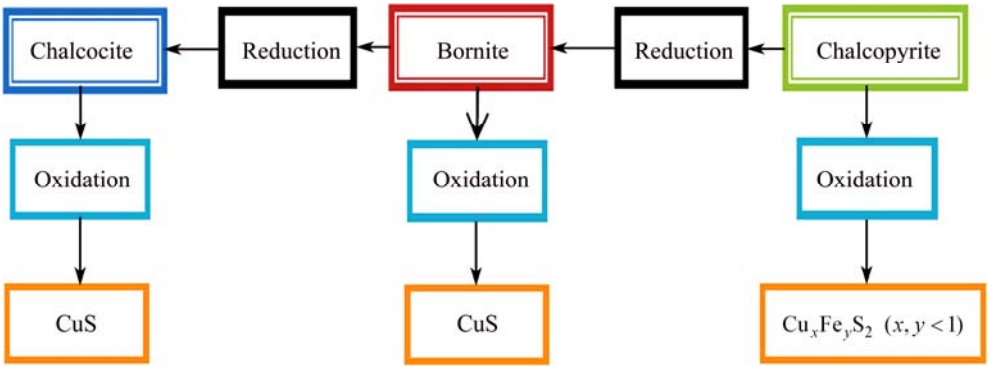


**Fig. 10** Dissolution models of chalcopyrite and bornite in acid culture medium

bornite by controlling the diffusion of ions [35,36].

For the chalcopyrite dissolution process, the electrochemical analysis reveals that the reaction rate of direct oxidation pathway was very low even at a relatively high redox potential. The other dissolution pathway of chalcopyrite can be described as a reduction−oxidation pathway, which contains reduction reactions and further oxidation reactions. During this dissolution pathway, chalcopyrite was initially reduced to bornite, and then was further oxidized along with the dissolution process of bornite. The electrochemical analysis definitely revealed that the dissolution of chalcopyrite can be significantly accelerated due to the reduction reactions, and the oxidation−reduction reactions of chalcopyrite and bornite electrodes were similar. Moreover, the detected product of covellite (CuS) by XPS analysis further supported this suggestion. Therefore, the dissolution pathway of continuous reduction−oxidation was preferred in this work.

Based on the above results, the main difficulty in effective dissolution of chalcopyrite is the initial reduction reaction, which was considered the main rate limiting step. The higher reaction rate of direct oxidation of bornite contributed to a higher copper extraction, and the further oxidation can be inhibited by the formation of covellite (CuS). Therefore, accelerating the initial reduction process of chalcopyrite and enhancing the dissolution of formed covellite (CuS) were conducive to the effective dissolution of chalcopyrite. And the enhancement of covellite (CuS) dissolution process can be a key to the effective dissolution of bornite.

## 4 Conclusions

1) The dissolution rate of bornite is significantly higher than that of chalcopyrite in acid culture medium mainly because of its relatively higher oxidation rate.

2) Chalcopyrite and bornite electrodes have similar electrochemical behaviors and similar dissolution processes. Covellite (CuS) is detected as the main intermediate species during both chalcopyrite and bornite dissolution processes.

3) The preferred dissolution pathway of bornite in acid culture medium is a direct oxidation process to covellite (CuS) and cupric ions. The preferred dissolution pathway of chalcopyrite in acid culture medium is a continuous reduction−oxidation process, in which chalcopyrite is initially reduced to bornite, and then oxidized to covellite (CuS).

4) The oxidation of formed covellite (CuS) may be one of the main limiting steps of the further dissolution of bornite. The initial reduction of chalcopyrite can be the main rate limiting step of chalcopyrite dissolution in acid culture medium.

## References

[1] VAUGHAN D J, CRAIG J R. Mineral chemistry of metal sulfides [M]. Cambridge: Cambridge University Press, 1978.

[2] KOTO K, MORIMOTO N. Superstructure investigation of bornite, $Cu_5FeS_4$, by the modified partial Patterson function [J]. Acta Crystallographica Section B: Structural Crystallography and Crystal Chemistry, 1975, 31(9): 2268−2273.

[3] DAVENPORT W G L, KING M, SCHLESINGER M, BISWAS A K. Extractive metallurgy of copper [M]. Amsterdam: Elsevier, 2002.

[4] VERA M, SCHIPPERS A, SAND W. Progress in bioleaching: Fundamentals and mechanisms of bacterial metal sulfide oxidation—Part A [J]. Applied Microbiology and Biotechnology, 2013, 97(17): 7529−7541.

[5] WATLING H. The bioleaching of sulphide minerals with emphasis on copper sulphides—A review [J]. Hydrometallurgy, 2006, 84(1): 81−108.

[6] BRIERLEY J, BRIERLEY C. Present and future commercial applications of biohydrometallurgy [J]. Hydrometallurgy, 2001, 59(2): 233−239.

[7] GHAHREMANINEZHAD A, DIXON D, ASSELIN E. Electrochemical and XPS analysis of chalcopyrite ($CuFeS_2$) dissolution in sulfuric acid solution [J]. Electrochimica Acta, 2012, 87: 97−112.

[8] YANG Yi, LIU Wei-hua, CHEN Miao. A copper and iron K-edge XANES study on chalcopyrite leached by mesophiles and moderate thermophiles [J]. Minerals Engineering, 2013, 48(1): 31−35.

[9] DREISINGER D, ABED N. A fundamental study of the reductive leaching of chalcopyrite using metallic iron. Part I: Kinetic analysis [J]. Hydrometallurgy, 2002, 66(1): 37−57.

[10] NAVA D, GONZ LEZ I. Electrochemical characterization of chemical species formed during the electrochemical treatment of chalcopyrite in sulfuric acid [J]. Electrochimica Acta, 2006, 51(25): 5295−5303.

[11] JIANG Lei, ZHOU Huai-yang, PENG Xiao-tong, DING Zhong-hao. The use of microscopy techniques to analyze microbial biofilm of the bio-oxidized chalcopyrite surface [J]. Minerals Engineering, 2009, 22(1): 37−42.

[12] SASAKI K, NAKAMUTA Y, HIRAJIMA T, TUOVINEN O. Raman characterization of secondary minerals formed during chalcopyrite leaching with *Acidithiobacillus ferrooxidans* [J]. Hydrometallurgy, 2009, 95(1): 153−158.

[13] PRICE D, CHILTON J. The anodic reactions of bornite in sulphuric acid solution [J]. Hydrometallurgy, 1981, 7(1): 117−133.

[14] PESIC B, OLSON F. Dissolution of bornite in sulfuric acid using oxygen as oxidant [J]. Hydrometallurgy, 1984, 12(2): 195−215.

[15] BEVILAQUA D, GARCIA O Jr, TUOVINEN O. Oxidative dissolution of bornite by *Acidithiobacillus ferrooxidans* [J]. Process Biochemistry, 2010, 45(1): 101−106.

[16] BEVILAQUA D, ACCIARI H A, ARENA F A, BENEDETTI A V, FUGIVARA C S, NIOR O G Jr. Utilization of electrochemical impedance spectroscopy for monitoring bornite ($Cu_5FeS_4$) oxidation by *Acidithiobacillus ferrooxidans* [J]. Minerals Engineering, 2009, 22(3): 254−262.

[17] QIN Wen-qing, WANG Jun, ZHANG Yan-sheng, ZHEN Shi-jie, SHANG He, LIU Qian, SHI Hai-bin, ZHANG Jian-wen, QIU Guan-zhou. Electrochemical behavior of massive bornite bioleached electrodes in the presence of *Acidithiobacillus ferrooxidans* and *Acidithiobacillus caldus* [J]. Advanced Materials Research, 2009, 71: 417−420.

[18] QIN Wen-qing, YANG Cong-ren, LAI Shao-shi, WANG Jun, LIU Kai, ZHANG Bo. Bioleaching of chalcopyrite by moderately thermophilic microorganisms [J]. Bioresource Technology, 2013, 129: 200−208.

[19] LIANG Chang-li, XIA Jin-lan, YANG Yi, NIE Zhen-yuan, ZHAO Xiao-juan, ZHENG Lei, MA Chen-yan, ZHAO Yi-dong. Characterization of the thermo-reduction process of chalcopyrite at 65 °C by cyclic voltammetry and XANES spectroscopy [J]. Hydrometallurgy, 2011, 107(1): 13−21.

[20] ACRES R G, HARMER S L, BEATTIE D A. Synchrotron XPS studies of solution exposed chalcopyrite, bornite, and heterogeneous chalcopyrite with bornite [J]. International Journal of Mineral Processing, 2010, 94(1): 43−51.

[21] ZHAO Hong-bo, WANG Jun, HU Ming-hao, QIN Wen-qing, ZHANG Yan-sheng, QIU Guan-zhou. Synergistic bioleaching of chalcopyrite and bornite in the presence of *Acidithiobacillus ferrooxidans* [J]. Bioresource Technology, 2013, 149: 71−76.

[22] GU Guo-hua, HU Ke-ting, ZHANG Xun, XIONG Xian-xue, YANG Hui-sha. The stepwise dissolution of chalcopyrite bioleached by *Leptospirillum ferriphilum* [J]. Electrochimica Acta, 2013, 103: 50−57.

[23] LI A-lin, HUANG Song-tao. Comparison of the electrochemical mechanism of chalcopyrite dissolution in the absence or presence of *Sulfolobus metallicus* at 70 °C [J]. Minerals Engineering, 2011, 24(13): 1520−1522.

[24] ARCE E M, GONZÁLEZ I. A comparative study of electrochemical behavior of chalcopyrite, chalcocite and bornite in sulfuric acid solution [J]. International Journal of Mineral Processing, 2002, 67(1): 17−28.

[25] LI Hong-xu, QIU Guan-zhou, HU Yue-hua, CANG Da-qiang, WANG Dian-zuo. Electrochemical behavior of chalcopyrite in presence of *Thiobacillus ferrooxidans* [J]. Transactions of Nonferrous Metals Society of China, 2006, 16(5): 1240−1245.

[26] LIANG Chang-li, XIA Jin-lan, NIE Zhen-yuan, LUO Xian-ping. Comparison of electrochemical behaviors of chalcopyrite, bornite, chalcocite and covellite in 9K medium [J]. Advanced Materials Research, 2013, 634: 68−71.

[27] MAJUSTE D, CIMINELLI V, OSSEO-ASARE K, DANTAS M, MAGALH ES-PANIAGO R. Electrochemical dissolution of chalcopyrite: Detection of bornite by synchrotron small angle X-ray diffraction and its correlation with the hindered dissolution process [J]. Hydrometallurgy, 2012, 111: 114−123.

[28] SANDSTR M Å, SHCHUKAREV A, PAUL J. XPS characterisation of chalcopyrite chemically and bio-leached at high and low redox potential [J]. Minerals Engineering, 2005, 18(5): 505−515.

[29] LEFEVRE G, WALCARIUS A, EHRHARDT J J, BESSIERE J. Sorption of iodide on cuprite ($Cu_2O$) [J]. Langmuir, 2000, 16(10): 4519−4527.

[30] PEISERT H, CHASS T, STREUBEL P, MEISEL A, SZARGAN R. Relaxation energies in XPS and XAES of solid sulfur compounds [J]. Journal of Electron Spectroscopy and Related Phenomena, 1994, 68: 321−328.

[31] BHIDE V, SALKALACHEN S, RASTOG A, RAO C, HEGDE M. Depth profile composition studies of thin film CdS: $Cu_2S$ solar cells using XPS and AES [J]. Journal of Physics D: Applied Physics, 1981, 14(9): 1647.

[32] NAKAI I, SUGITANI Y, NAGASHIMA K, NIWA Y. X-ray photoelectron spectroscopic study of copper minerals [J]. Journal of Inorganic and Nuclear Chemistry, 1978, 40(5): 789−791.

[33] DESCOSTES M, MERCIER F, THROMAT N, BEAUCAIRE C, GAUTIER-SOYER M. Use of XPS in the determination of chemical environment and oxidation state of iron and sulfur samples: Constitution of a data basis in binding energies for Fe and S reference compounds and applications to the evidence of surface species of an oxidized pyrite in a carbonate medium [J]. Applied Surface Science, 2000, 165(4): 288−302.

[34] LI Y, KAWASHIMA N, LI J, CHANDRA A, GERSON A. A review of the structure, and fundamental mechanisms and kinetics of the leaching of chalcopyrite [J]. Advances in Colloid and Interface Science, 2013, 197: 1−32.

[35] SMART R S C, SKINNER W M, GERSON A R. XPS of sulphide mineral surfaces: Metal-deficient, polysulphides, defects and elemental sulphur [J]. Surface and Interface Analysis, 1999, 28(1): 101−105.

[36] HACKL R, DREISINGER D, PETERS E, KING J. Passivation of chalcopyrite during oxidative leaching in sulfate media [J]. Hydrometallurgy, 1995, 39(1): 25−48.

# 黄铜矿与斑铜矿在酸性细菌培养基中的电化学溶解对比

赵红波[1,2]，胡明皓[1,2]，李祷旎[1,2]，朱 珊[1,2]，覃文庆[1,2]，邱冠周[1,2]，王 军[1,2]

1. 中南大学 资源加工与生物工程学院，长沙 410083；
2. 中南大学 生物冶金教育部重点实验室，长沙 410083

**摘 要**：采用电化学测试和 X 射线光电子能谱(XPS)测试分析黄铜矿与斑铜矿在酸性细菌培养基中的电化学溶解过程。斑铜矿直接氧化反应比还原反应更容易发生，但黄铜矿既难被氧化，又难被还原。斑铜矿具有更高的氧化速率，从而比黄铜矿更容易被溶解。铜蓝(CuS)是黄铜矿与斑铜矿溶解过程的中间产物。因此，斑铜矿的溶解途径主要为直接氧化过程，中间产物铜蓝(CuS)可能限制其进一步溶解。黄铜矿的溶解途径包含了还原−氧化过程，其中，黄铜矿首先被还原为与斑铜矿类似的中间产物，再进一步被氧化，并产生铜蓝(CuS)，而黄铜矿的最初还原过程是其溶解过程的主要限制步骤。

**关键词**：黄铜矿；斑铜矿；电化学溶解；酸性培养基；细菌浸出

**(Edited by Yun-bin HE)**